Inorganic Chemistry
Cite This: Inorg. Chem. XXXX, XXX, XXX–XXX
Article
pubs.acs.org/IC

Magnetic and Structural Studies of G-Phase Compound $Mn_6Ni_{16}Si_7$

Sheikh Jamil Ahmed,[†] John E. Greedan,[‡,§] Chad Boyer,[∥] and Marek Niewczas*[,†,§]

[†]Department of Materials Science and Engineering, [‡]Department of Chemistry, and [§]Brockhouse Institute of Materials Research, McMaster University, Hamilton, Ontario L8S 4L8, Canada

[∥]Canadian Neutron Beam Centre, Canadian Nuclear Laboratories, Chalk River, Ontario K0J 1J0, Canada

Supporting Information

ABSTRACT: Transition metal compounds with complex crystal structures tend to demonstrate interesting magnetic coupling resulting in unusual magnetic properties. In this work, the structural and magnetic characterization of a single crystal of the Ni–Mn–Si based G-phase compound, $Mn_6Ni_{16}Si_7$, grown by the Czochralski method, is reported. In this structure, isolated octahedral Mn_6 clusters form an fcc lattice. As each octahedron consists of eight edge-sharing equilateral triangles, the possibility for geometric frustration exists. Magnetization and specific heat measurements showed two magnetic phase transitions at 197 and 50 K, respectively. At 100 K neutron diffraction on powder samples shows a magnetic structure with $k = (001)$ in which only four of the six Mn spins per cluster order along ⟨100⟩ directions giving a two-dimensional magnetic structure consistent with intracluster frustration. Below the 50 K phase transition, the Mn spin-cants away from ⟨100⟩ directions, and a weak moment develops on the two remaining Mn octahedral sites.

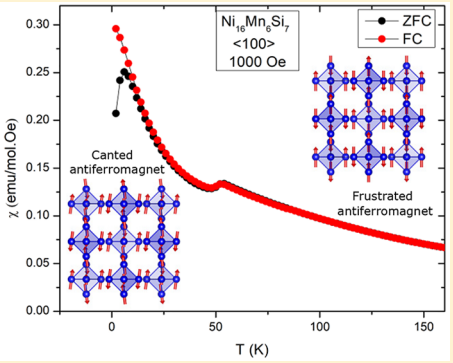

INTRODUCTION

The geometry of the crystal structure and strong nearest neighbor interactions in compounds containing transition metal ions give rise to phenomena such as geometric frustration, noncollinear magnetism and the coupling of these properties.[1−5] The compounds display new magnetic properties including canted ferromagnetic state,[6−12] non-collinear ferrimagnetism,[13] metamagnetism,[14] giant magnetostriction,[15,16] unusual magnetic hysteresis behavior,[17] and giant magnetoresistance,[18] among others. The enhanced magnetic interactions make these materials prominent candidates for applications in quantum computation, data storage, magnetic refrigeration, and spintronics.[19−23]

The G-phase-based compounds crystallize in a $Mg_6Cu_{16}Si_7$ (ternary) or Th_6Mn_{23} (binary) type structure. The system consists of a complex network of octahedra and supertetrahedra with at least one of the constituting elements being a transition metal.[24,25] Several studies of these systems have focused primarily on the properties associated with high density magnetic information recording media, magnetic suppression and superconductivity.[25−30] However, a complex crystal structure containing transition metals holds promises for unique magnetic coupling that can give rise to multifunctional behavior in these compounds.

The Ni–Mn–Si based $Mn_6Ni_{16}Si_7$ type G-phase was proposed to be an antiferromagnetic system below 200 K by Stadnik and Skolozdra.[31] Further neutron diffraction and magnetization analysis by Kolenda et al.[32] resulted in a proposed magnetic structure in which all Mn spins are ordered below 200 K with a moment of 2.7 μ_B/Mn atom at 80 K, the base temperature of their study. Nonetheless, some aspects of the physical properties of the system seem inconsistent with this model, for example the magnetic susceptibility increases as the temperature decreases below T_N which deviates from conventional antiferromagnetic behavior in a polycrystalline system.

In the present work, comprehensive studies of the magnetic properties of a $Mn_6Ni_{16}Si_7$ single crystal grown by the Czochralski method as well as neutron diffraction on a powder sample are presented. The temperature range of the measurements is extended to 2 K. The emergence of an additional low-temperature phase transition below 50 K is reported. Magnetic structures refined at 100 and 3.5 K from the neutron data are found to be more consistent with the bulk susceptibility data and the presence of geometric frustration. We discuss the possible changes in the magnetic structure of $Mn_6Ni_{16}Si_7$ compound in terms of the magnetic susceptibility measurements.

EXPERIMENTAL DETAILS

The $Mn_6Ni_{16}Si_7$ single crystal was grown by the Czochralski crystal growth method under an argon atmosphere using the RF heating. High-purity Ni (99.95%), Mn (99.98%), and Si (99.999%) were melted in an alumina crucible, and the crystal was pulled using a tungsten wire seed with a constant pulling rate of 0.5 mm/min and 30 rpm rotation. The growth direction was found to be along ⟨110⟩ from Laue X-ray data. Preoriented samples of 2 mm × 2 mm × 2 mm were spark-cut from the as-grown crystal and used for magnetic and specific heat measurements.

Studies of the magnetic properties were conducted with a Quantum Design MPMS SQUID magnetometer. The zero field cooled (ZFC)–field cooled (FC) magnetic susceptibly measurements were carried out from 350 to 2 K on an oriented single crystal with a constant

Received: July 19, 2018

DOI: 10.1021/acs.inorgchem.8b01964
Inorg. Chem. XXXX, XXX, XXX–XXX

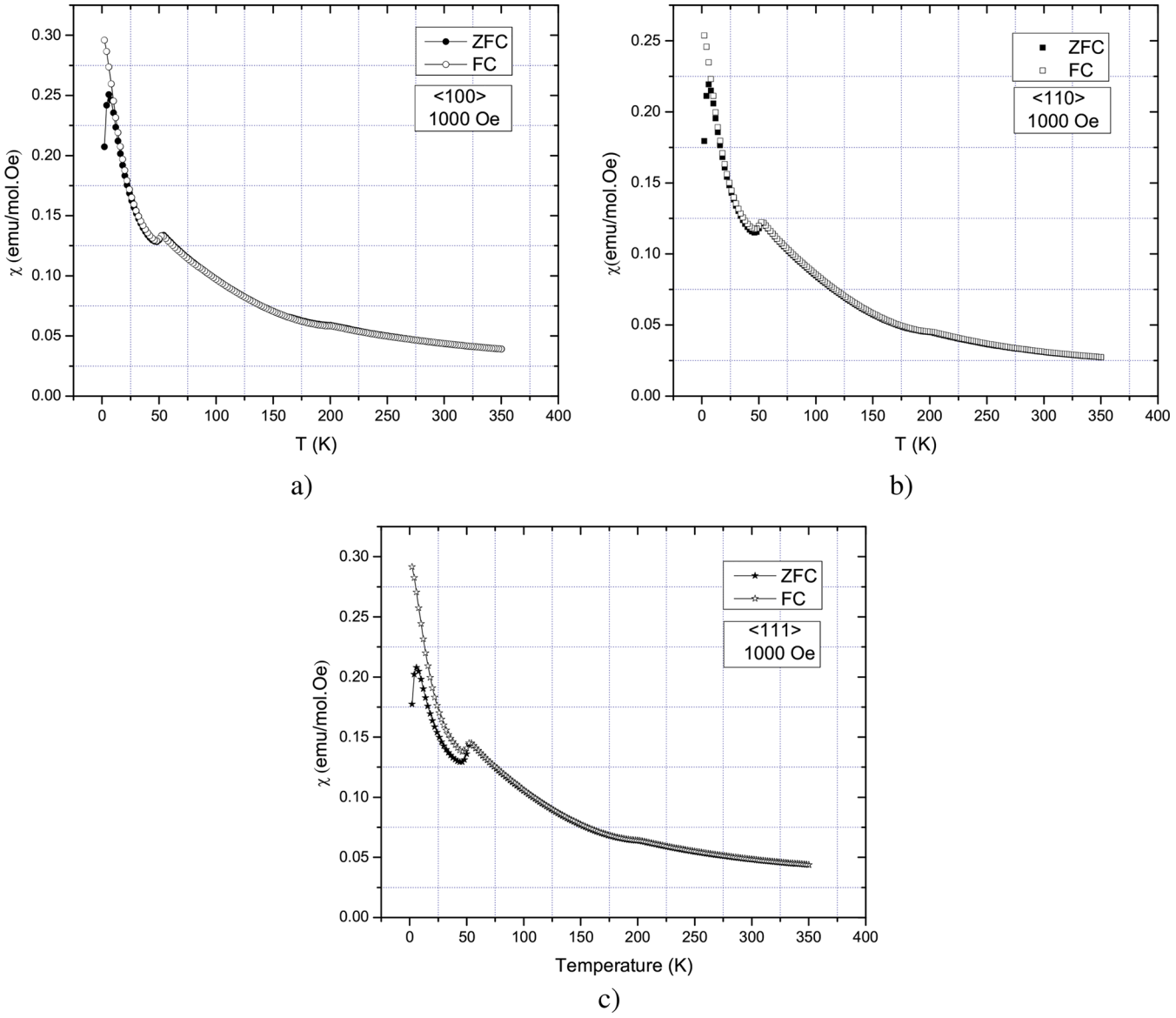

Figure 1. (a) ZFC-FC magnetic susceptibility of $Mn_6Ni_{16}Si_7$ crystal at 1000 Oe field applied along (a) ⟨100⟩, (b) ⟨110⟩, and (c) ⟨111⟩.

magnetic field of 1000 Oe applied in ⟨100⟩, ⟨110⟩, and ⟨111⟩ directions.

The heat capacity of the compound was measured from 2 to 303 K using the Quantum Design PPMS system on the same 2 mm × 2 mm × 2 mm crystal samples used in magnetic studies.

The neutron diffraction studies of the $Mn_6Ni_{16}Si_7$ compound were performed at the Canadian Neutron Beam Centre in Chalk River on the C2 High-Resolution Powder Diffractometer with a wavelength of 1.33 Å. The diffraction data were collected on about 4 g of the powdered $Mn_6Ni_{16}Si_7$ sample, sealed in a thin-walled vanadium tube under argon atmosphere. The powder was obtained from a larger polycrystalline ingot, prepared by arc-melting of the pure elements under argon atmosphere. To improve homogeneity, the ingot was remelted three times. Excess Mn was added to compensate for the evaporation loss of the element. The compound was then sealed in an evacuated silica tube, annealed at 800 °C for 2 weeks, and subsequently, quenched in ice water mixture to further improve the crystallinity. No mass loss was observed due to annealing. Phase purity was confirmed by X-ray powder diffraction using a PANalytical X'Pert Pro diffractometer with Co $K\alpha_1$ radiation (refinement profile shown in Figure S1 of supplementary data).

Refinement of the diffraction data was performed using the full-profile Rietveld method implemented in the FullProf program.[33−35] The magnetic configurations were generated with the representation analysis program SARAh.[36]

RESULTS

Magnetic Susceptibility. Figure 1 shows ZFC-FC magnetic susceptibly between 2 and 350 K under the constant magnetic field of 1000 Oe applied along ⟨100⟩, ⟨110⟩, and ⟨111⟩ directions of the crystal. The data clearly showed two transitions at ∼50 and 197 K, the latter in agreement with Kolenda et al.[32] Additionally, one observes a ZFC/FC divergence below 6 K suggesting a weak spin-freezing effect. Thus, two new anomalies are discovered here below the 80 K base temperature of the earlier studies. A comparison of the ⟨100⟩, ⟨110⟩, and ⟨111⟩ ZFC-FC data (Figure S2) showed a inconsistent anisotropic behavior of ZFC and FC magnetic susceptibility which indicates the applied field of 1000 Oe is too small to capture any magnetic anisotropy.

Further analysis of the data with the field cooled Fisher heat capacity,[37] $d(\chi T)/dT$ versus T plot in Figure 2a, showed two of the transitions (50 (1) K and 197 (1) K) quite clearly.

DOI: 10.1021/acs.inorgchem.8b01964
Inorg. Chem. XXXX, XXX, XXX−XXX

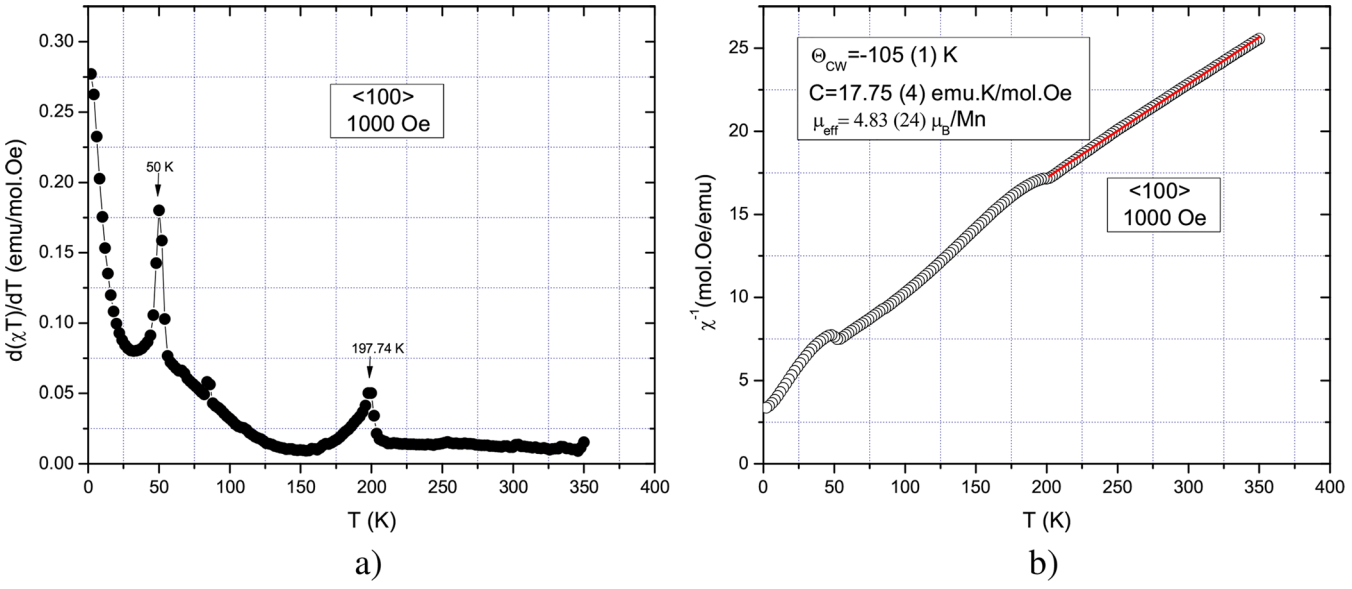

Figure 2. (a) FC d(χT)/dT vs T plot identifying the transition temperatures, for crystal with the applied field along the ⟨100⟩ direction. (b) Curie–Weiss fit on the inverse susceptibility data of $Mn_6Ni_{16}Si_7$ single crystals along ⟨100⟩ above 200 K.

The true Néel temperature was identified to be 197 (1) K from the second peak of the graph.

From the inverse FC susceptibly plot along the ⟨100⟩ crystal direction, a Curie–Weiss fitting was done above 197 K (Figure 2b). The Curie constant, C of 17.75 (4) emu K/mol Oe yielded an effective magnetic moment per Mn atom, μ_{eff}/Mn of 4.83 (24) μ_B which is very close to the effective moment for of 4.90 μ_B for Mn^{3+} (S = 2) compared to the 5.91 μ_B for Mn^{2+} ($S = \frac{5}{2}$). The Curie–Weiss parameters for FC susceptibility in other directions are listed in Table S1 of supplementary data. Some caution should be taken as this fitting region may not be strictly in the paramagnetic regime. The Curie–Weiss temperature, Θ_{CW} was estimated to be −105 (1) K, which indicates the presence of a strong antiferromagnetic exchange. Moreover, the susceptibility data continue to increase with decreasing temperature, indicating a persistent paramagnetic contribution which is likely due to the presence of geometrically frustrated paramagnetic ions.

Heat Capacity Measurement. Figure 3a shows the heat capacity of $Mn_6Ni_{16}Si_7$ measured under zero magnetic field between 2 and 303 K. The data clearly depict a λ anomaly peak at 197 K that corresponds to a transition between antiferromagnetic and paramagnetic states. A second transition at 50 K characterized by a weak, almost undetectable peak in heat capacity data (inset in Figure 3a), is consistent with the transition observed in the magnetic susceptibility plots in Figure 1. To obtain the magnetic contribution to the heat capacity of $Mn_6Ni_{16}Si_7$ one needs to subtract that of a suitable lattice match, normally a paramagnetic iso-structural compound.[38] A previous study of the magnetic properties of $Ti_6Ni_{16}Si_7$ showed a Pauli paramagnetic-like behavior,[25] which was also observed in our measurements of magnetic susceptibility of the compound under an applied magnetic field of 1000 Oe (Figure S3). However, the heat capacity as a function of temperature showed a cusp at 140 K for $Ti_6Ni_{16}Si_7$ (closed circles in Figure 3a), which is an indication of a phase transition, nevertheless unexpected, given the data of Holman et al.[25] and our magnetic measurements. The origin of this anomaly is unclear at present, but apart from this feature, $Ti_6Ni_{16}Si_7$ appeared to be a reasonable lattice match. Consequently, the magnetic contribution of the heat capacity for $Mn_6Ni_{16}Si_7$ was obtained (Figure 3b) by a direct subtraction of the $Ti_6Ni_{16}Si_7$ data. Note that the 50 K anomaly is now clearly evident. Furthermore, a linear fitting of C_{mag} was obtained below 6 K (inset in Figure 3b. Such a linear dependence of heat capacity is usually a sign of spin-freezing[7] which further supports the cusp at 6 K to be associated with such an anomaly.

Neutron Diffraction. Neutron diffraction data were obtained on a polycrystalline powder sample at 298, 100, and 4 K, corresponding to the three different regimes of magnetic susceptibility and heat capacity behavior. As indicated by magnetic measurement, at room temperature the structure was refined to be a paramagnetic type with no additional magnetic contribution (Figure 4a). The room-temperature structure was refined by the Rietveld method (Figure 4a), and the structural parameters are listed in Table 1. The structural parameters were found to be in excellent agreement with previously reported results for $Mn_6Ni_{16}Si_7$.[31,32,39] The occupancies of individual elements were kept constant during the refinement. The Mn atoms occupy the sites of regular octahedra which are not directly connected with other octahedra. Each Mn atom within an octahedron is coupled with four nearest neighbors by exchange constant J_1, one next-nearest neighbor by J_2, and with four neighbors of the adjacent octahedra by J_3, as shown in Figure 5. The J_1, J_2, and J_3 pathway lengths are approximately 0.279a, 0.393a, and 0.429a, respectively, where a is the lattice constant.

The neutron diffraction data collected at 100 K show new reflections, relative to room temperature, which can be indexed as (210), (310), (320), and (312). These reflections are systematically absent in $Fm\bar{3}m$ symmetry structure and can thus be associated with magnetic ordering. The same reflections were reported by Kolenda et al.[32] in their studies of the compound.

The solution of the magnetic structure was based on the representation analysis method using SARAh.[36] For the ordering wave vector k = (0 0 1) four basis vectors Γ_2, Γ_3, Γ_9, and Γ_{10} resulted from this approach. The best refinement was obtained using Γ_9 (refinement parameters for all Γ configurations are

DOI: 10.1021/acs.inorgchem.8b01964
Inorg. Chem. XXXX, XXX, XXX−XXX

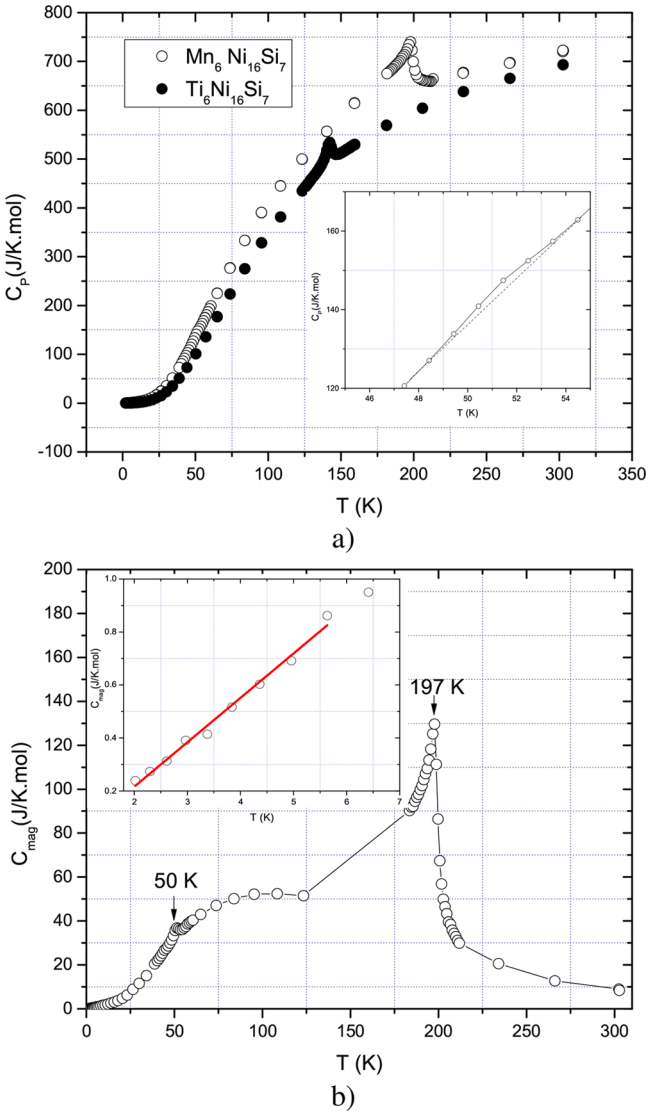

Figure 3. (a) Zero magnetic field heat capacity of $Mn_6Ni_{16}Si_7$ (open circles) and the lattice match compound $Ti_6Ni_{16}Si_7$ (closed circles) from 2 to 303 K. $Mn_6Ni_{16}Si_7$ shows a weak transition at 50 K, which is magnified in the inset and a sharp antiferromagnetic to paramagnetic transition at 198 K. $Ti_6Ni_{16}Si_7$ also undergoes a transition at 142 K. (b) Magnetic contribution, C_{mag}, for $Mn_6Ni_{16}Si_7$ as a function of temperature. The magnetic contribution C_{mag} is obtained by direct subtraction of the lattice match compound $Ti_6Ni_{16}Si_7$ data ignoring the phase transition. A linear fitting of C_{mag} below 6 K (magnified in the inset) supports the spin-freezing anomaly.

listed in Table S2). The Rietveld refinement profile is shown in Figure 4b, and magnetic moments are listed in Table 1. The resulting magnetic structure (Figure 6) shows a 2D antiferromagnetic configuration of Mn^{2+} atoms involving only four of the six sites on the Mn_6 octahedron oriented along ⟨100⟩ directions in an *ab* plane. Here, Mn occupancy is separated into 2 Mn sublattices, Mn−I and Mn−II. Mn−I contain chains of atoms on a principal plane arranged antiferromagnetically with the nearest neighbor atoms. Mn−II atoms lie on top and bottom of the Mn−I chains and remain paramagnetic providing evidence of spin frustration within each octahedron. It can be seen that two of four J_1 Mn are coupled antiferromagnetically, while the remaining two are paramagnetic. Mn atoms connected by J_2 are coupled ferromagnetically as would be required given dominant nearest neighbor antiferromagnetic exchange. It can also be noticed that two-dimensional planes formed by the ordered Mn ions are coupled antiferromagnetically with each other indicating strong antiferromagnetism in $Mn_6Ni_{16}Si_7$. The Mn−I moments were refined to be 4.45 (5) μ_B per Mn ion. It can be seen that the moment is close to the theoretical and experimentally reported value for Mn^{2+}, i.e., 5 μ_B (with $g = 2$ and $S = \frac{5}{2}$) and 4.7 μ_B,[1] respectively. The moment for the Ni ions were refined to be 0 to within 2σ. It can be seen that our model is different from the one proposed by Kolenda et al.[32] Refinement of the 100 K data using their proposed magnetic structure showed relatively poor agreement with the observed powder pattern (Table S2, Figure S4). However, our model of Figure 6, with frustrated Mn spins, is consistent with the observed bulk susceptibility data which shows a paramagnetic like contribution persisting below T_N = 198 K.

A careful comparison of neutron diffraction at 4 and 100 K revealed an extra (100) peak at 4 K (Figure 4d). The presence of such a reflection implies the magnetic moments cannot be parallel to (100). Consequently, it can be presumed that the 2D antiferromagnetic symmetry is broken. This result can be associated with the phase transition at 50 K. The refinement showed that the Mn−I moment value at 4 K is increased slightly to 4.74 (11) μ_B and that the spins make a canting angle with respect to (100) of 9 (1°) (Figure 7). This is sometimes called hidden spin-canting which refers to a configuration where the moments of multiple sublattices are canted about the axis but still in a collinear arrangement.[40−43] Note that the moments are still consistent with values for the $S = \frac{5}{2}$ system.[1] Also, a small moment of 0.65 (24) μ_B appears on the Mn−II site which may be real. Note that even below 50 K, the model predicts a high concentration of paramagnetic spins, consistent with the bulk susceptibility which continues to increase at lower temperatures. The relevant refinement parameters are shown in Table 1, and the Rietveld profile is show in Figure 4c.

Table 1. Refined Structural Parameters for $Mn_6Ni_{16}Si_7$

temperature	298 K	100 K	4 K
lattice constant (Å)	11.1497(4)	11.1238(3)	11.1198(4)
space group	$Fm\bar{3}m$	$Fm\bar{3}m$	$Fm\bar{3}m$
magnetic phase	paramagnetic	antiferromagnetic	canted antiferromagnetic
Mn; 24e (x, 1/2, 1/2)	0.6969(3)	0.6969(3)	0.6969(3)
B(Mn) (Å^2)	0.49(15)	0.32(14)	0.09(5)
M(Mn−I) (μ_B)		4.45(5)	4.74(11)
M(Mn−II) (μ_B)		0	0.65(24)
Ni1; 32f (x, x, x)	0.33322(11)	0.33322(11)	0.33322(11)
B(Ni1) (Å^2)	0.58(5)	0.36(5)	0.22(5)
M(Ni1) (μ_B)		0	0
Ni2; 32f (x, x, x)	0.11780(12)	0.11780(12)	0.11780(12)
B(Ni2) (Å^2)	0.58(5)	0.49(5)	0.36(5)
M(Ni2)(μ_B)		0	0
Si1; 4a (1/2, 1/2, 0)			
B(Si1) (Å^2)	0.48(10)	0.74(27)	0.66(28)
Si2; 24e (1/2, 1/4, 1/4)			
B(Si2) (Å^2)	0.48(10)	0.35(10)	0.34(10)
χ^2	5.33	9.66	10.4
R_{wp}	11.4	10.3	10.7
R_F	2.51	1.66	1.94
R_{mag}		8.81	8.06

DOI: 10.1021/acs.inorgchem.8b01964
Inorg. Chem. XXXX, XXX, XXX−XXX

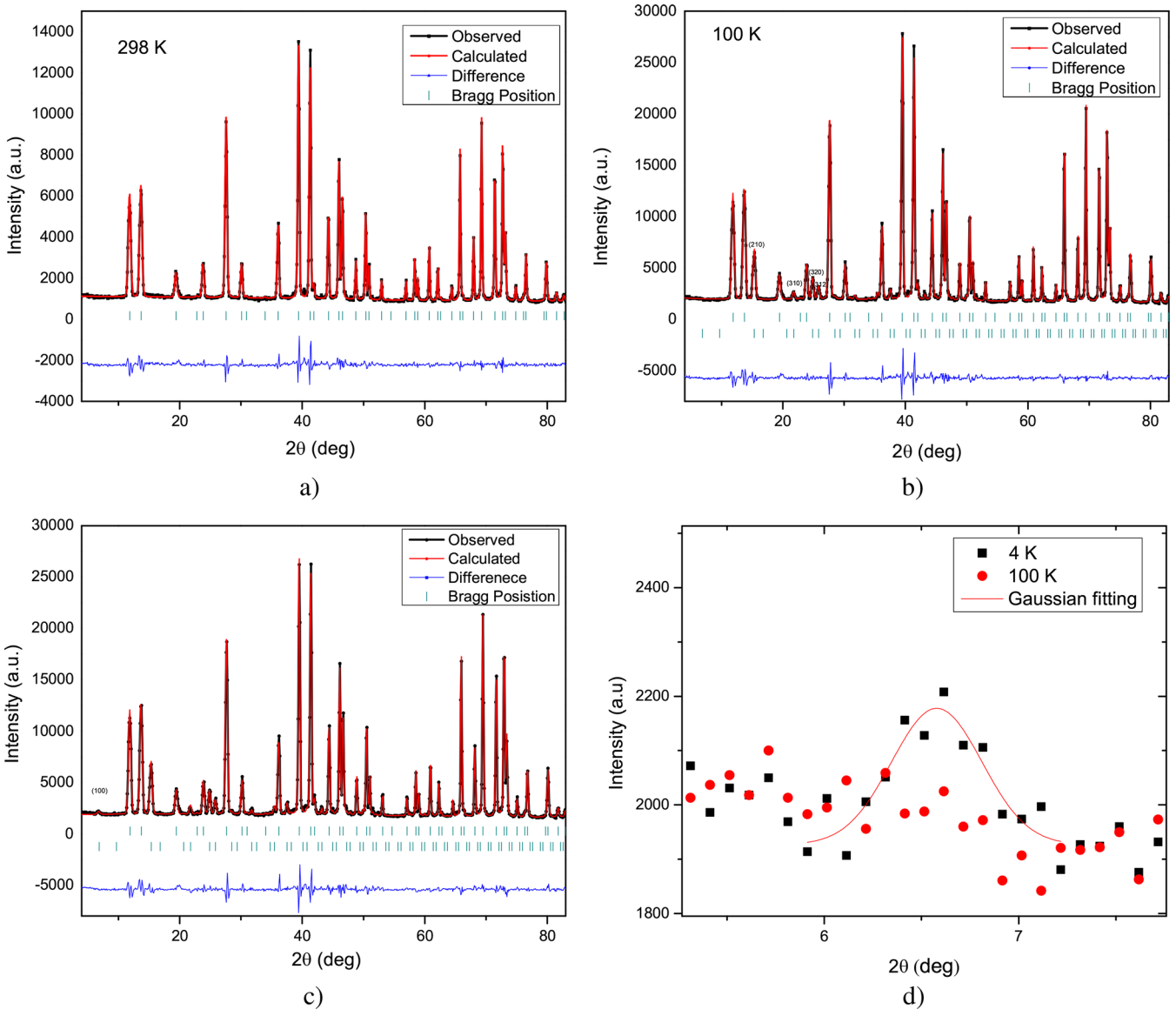

Figure 4. Rietveld refinement of the neutron powder diffraction data at (a) 298 K, (b) 100 K, and (c) 4 K. (d) Comparison of 4 and 100 K neutron data at low 2θ, showing (100) peak at 4 K.

DISCUSSION

The observation of the magnetic susceptibility and heat capacity data suggesting a paramagnetic system above 197 K is reflected well in the neutron refinement at 298 K where no magnetic ordering of the $Mn_6Ni_{16}Si_7$ system was observed. The magnetic structure obtained in the 100 K refinement found Mn−II ions to be remaining as paramagnetic, while Mn−I atoms are antiferromagnetically coupled suggesting the system be a 2D geometrically frustrated antiferromagnet. The configuration can be related to the magnetic susceptibility data from 197 to 50 K, although the negative Θ_{CW} from the Curie−Weiss fitting of the inverse susceptibility confirmed the system to be antiferromagnetic below 197 K. Also, the magnetic susceptibility data consisted of a paramagnetic contribution that can be explained in terms of geometrically frustrated Mn−II atoms. The refinement at 4 K showed the breaking of the two-dimensional symmetry yielding a hidden spin-canted magnetic configuration. The structure can be associated with the phase transition at 50 K detected by the magnetic susceptibility and heat capacity measurement. The system also demonstrates another phase anomaly below 6 K, due to the spin-freezing effect. Although the refinement at 4 K found the Mn−II to be ordering with small moments, the system still contains higher concentrations of paramagnetic Mn ions. It is quite possible that freezing of these weak moments can result in the rapid drop of ZFC magnetization below 6 K. Such a weak phenomenon, however, can not be detected by the neutron diffraction experiments.

CONCLUSIONS

In this work, it has been shown that $Mn_6Ni_{16}Si_7$ shows remarkably complex magnetic behavior. Three phase transitions occur upon cooling from ambient temperature. Below 197 K, long-range antiferromagnetic order occurs but only with 2/3 of the Mn spins involved, which can be understood in terms of geometric magnetic frustration within the Mn_6 octahedra. The Mn moments are oriented along the ⟨100⟩ direction in a planar pattern. Below 50 K, these ordered moments cant away from ⟨100⟩ by an angle of 9° but remain collinear.

DOI: 10.1021/acs.inorgchem.8b01964
Inorg. Chem. XXXX, XXX, XXX−XXX

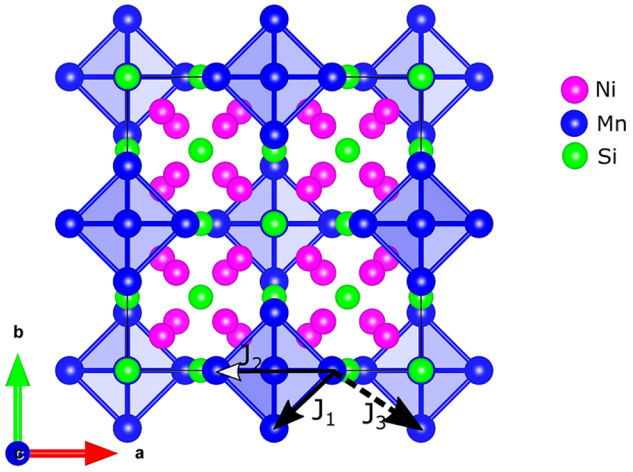

Figure 5. Refined crystal structure in the paramagnetic state. In the structure, Mn ions are connected by $4J_1$, $1J_2$, and $4J_3$ bonds.

Simultaneously, the previously paramagnetic Mn sites develop a small moment of 0.6 μ_B, compared with 4.70 μ_B found on the other Mn atoms. Finally, below 6 K, there is evidence of spin-freezing involving the remaining paramagnetic Mn spins.

■ ASSOCIATED CONTENT

Supporting Information

The Supporting Information is available free of charge on the ACS Publications website at DOI: 10.1021/acs.inorgchem.8b01964.

XRD powder refinement of $Mn_6Ni_{16}Si_7$, FC Curie–Weiss parameters anisotropy, ZFC magnetic susceptibility of lattice match compound $Ti_6Ni_{16}Si_7$, magnetic refinement parameters with different Γ configurations, Rietveld refinement with the magnetic structure model proposed by Kolenda et al.[32] (PDF)

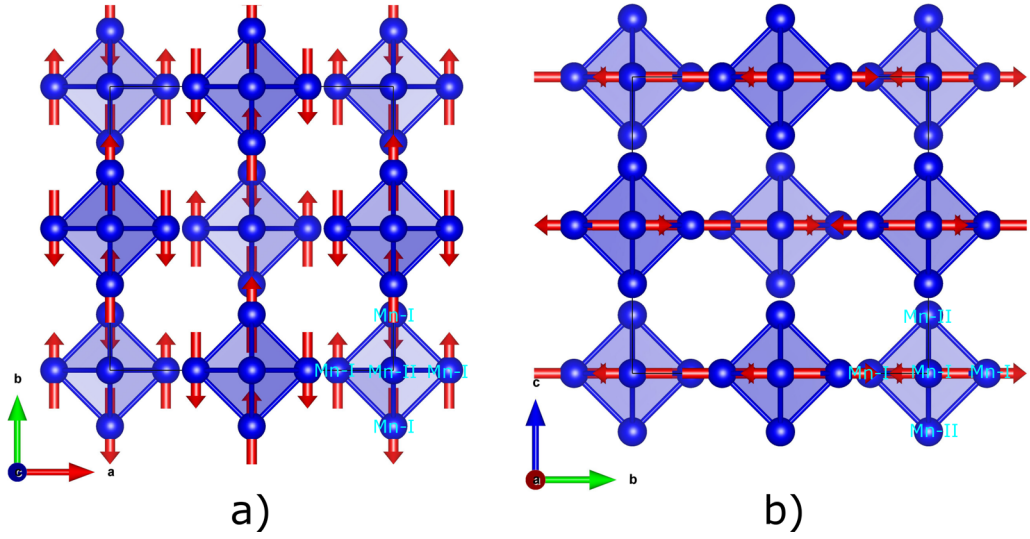

Figure 6. Magnetic structure at 100 K showing a two-dimensional (2D) magnetic arrangement magnetic moments between Mn–I ions (parallel to *ab* plane in the current coordinate system). Mn–II ions remain frustrated. The structures shown in the figure represent projection along the (a) *ab* and (b) *bc* planes, respectively.

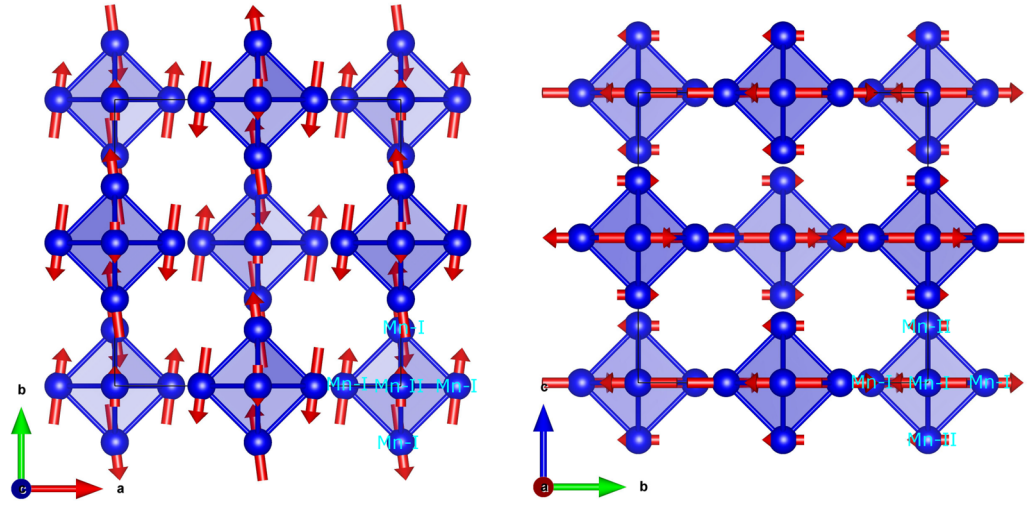

Figure 7. Hidden spin-canted antiferromagnetic structure is favored at 4 K. The two-dimensional magnetic symmetry is broken, and the moments are canted in (*ab*) plane. Magnetic moment vectors are guide to eye only. The structures presented in the figure corresponds to projection along the (a) *ab* and (b) *bc* planes, respectively.

DOI: 10.1021/acs.inorgchem.8b01964
Inorg. Chem. XXXX, XXX, XXX–XXX

AUTHOR INFORMATION

Corresponding Author

*E-mail: niewczas@mcmaster.ca.

ORCID

John E. Greedan: 0000-0003-1307-8379

Marek Niewczas: 0000-0002-8529-7194

Notes

The authors declare no competing financial interest.

ACKNOWLEDGMENTS

We thank Dr. A. S. Wills (University College London) for stimulating discussions. Dr. A. Dabkowski (McMaster University) assisted with the crystal growth process. Financial support of Natural Sciences and Engineering Research Council of Canada under the NSERC grant: "Artificially Structured Multiferroic Composites based on the Heusler alloys" is gratefully acknowledged.

REFERENCES

(1) Fries, T.; Shapira, Y.; Palacio, F.; Morón, M. C.; McIntyre, G. J.; Kershaw, R.; Wold, A.; McNiff, E.; et al. Magnetic ordering of the antiferromagnet Cu 2 MnSnS 4 from magnetization and neutron-scattering measurements. *Phys. Rev. B: Condens. Matter Mater. Phys.* **1997**, *56*, 5424.

(2) Hur, N.; Park, S.; Sharma, P.; Ahn, J.; Guha, S.; Cheong, S. Electric polarization reversal and memory in a multiferroic material induced by magnetic fields. *Nature* **2004**, *429*, 392.

(3) Ye, F.; Fernandez-Baca, J. A.; Fishman, R. S.; Ren, Y.; Kang, H.; Qiu, Y.; Kimura, T. Magnetic interactions in the geometrically frustrated triangular lattice antiferromagnet CuFeO 2. *Phys. Rev. Lett.* **2007**, *99*, 157201.

(4) Melchy, P.-É.; Zhitomirsky, M. Interplay of anisotropy and frustration: Triple transitions in a triangular-lattice antiferromagnet. *Phys. Rev. B: Condens. Matter Mater. Phys.* **2009**, *80*, 064411.

(5) Deng, S.; Sun, Y.; Wang, L.; Shi, Z.; Wu, H.; Huang, Q.; Yan, J.; Shi, K.; Hu, P.; Zaoui, A.; et al. Frustrated Triangular Magnetic Structures of Mn3ZnN: Applications in Thermal Expansion. *J. Phys. Chem. C* **2015**, *119*, 24983−24990.

(6) Fruchart, D.; Bertaut, E. F. Magnetic studies of the metallic perovskite-type compounds of manganese. *J. Phys. Soc. Jpn.* **1978**, *44*, 781−791.

(7) Ramirez, A. Strongly geometrically frustrated magnets. *Annu. Rev. Mater. Sci.* **1994**, *24*, 453−480.

(8) Greedan, J. E. Geometrically frustrated magnetic materialsBasis of a presentation given at Materials Discussion No. 3, 26−29 September, 2000, University of Cambridge, UK. *J. Mater. Chem.* **2001**, *11*, 37−53.

(9) Yu, M.-H.; Lewis, L.; Moodenbaugh, A. Large magnetic entropy change in the metallic antiperovskite Mn 3 GaC. *J. Appl. Phys.* **2003**, *93*, 10128−10130.

(10) Greedan, J. E. Frustrated rare earth magnetism: Spin glasses, spin liquids and spin ices in pyrochlore oxides. *J. Alloys Compd.* **2006**, *408-412*, 444−455.

(11) Yang, E.-C.; Liu, Z.-Y.; Wu, X.-Y.; Chang, H.; Wang, E.-C.; Zhao, X.-J. Co II, Mn II and Cu II-directed coordination polymers with mixed tetrazolate−dicarboxylate heterobridges exhibiting spin-canted, spin-frustrated antiferromagnetism and a slight spin-flop transition. *Dalton Trans* **2011**, *40*, 10082−10089.

(12) Matan, K.; Bartlett, B.; Helton, J.; Sikolenko, V.; Mat'aš, S.; Prokeš, K.; Chen, Y.; Lynn, J. W.; Grohol, D.; Sato, T.; et al. Dzyaloshinskii-Moriya interaction and spin reorientation transition in the frustrated kagome lattice antiferromagnet. *Phys. Rev. B: Condens. Matter Mater. Phys.* **2011**, *83*, 214406.

(13) Yan, J.; Sun, Y.; Wu, H.; Huang, Q.; Wang, C.; Shi, Z.; Deng, S.; Shi, K.; Lu, H.; Chu, L. Phase transitions and magnetocaloric effect in Mn3Cu0. 89N0. 96. *Acta Mater.* **2014**, *74*, 58−65.

(14) Dendrinou-Samara, C.; Walsh, J. P.; Muryn, C. A.; Collison, D.; Winpenny, R. E.; Tuna, F. Evidence of Spin Canting, Metamagnetism, Negative Coercivity and Slow Relaxation in a Two-Dimensional Network of {Mn6} Cages. *Eur. J. Inorg. Chem.* **2018**, *2018*, 485−492.

(15) Shimizu, T.; Shibayama, T.; Asano, K.; Takenaka, K. Giant magnetostriction in tetragonally distorted antiperovskite manganese nitrides. *J. Appl. Phys.* **2012**, *111*, 07A903.

(16) Shibayama, T.; Takenaka, K. Giant magnetostriction in antiperovskite Mn3CuN. *J. Appl. Phys.* **2011**, *109*, 07A928.

(17) Sun, Y.; Guo, Y.; Tsujimoto, Y.; Wang, C.; Li, J.; Wang, X.; Feng, H. L.; Sathish, C. I.; Matsushita, Y.; Yamaura, K. Unusual magnetic hysteresis and the weakened transition behavior induced by Sn substitution in Mn3SbN. *J. Appl. Phys.* **2014**, *115*, 043509.

(18) Kamishima, K.; Goto, T.; Nakagawa, H.; Miura, N.; Ohashi, M.; Mori, N.; Sasaki, T.; Kanomata, T. Giant magnetoresistance in the intermetallic compound Mn 3 GaC. *Phys. Rev. B: Condens. Matter Mater. Phys.* **2000**, *63*, 024426.

(19) Stamp, P. C.; Gaita-Arino, A. Spin-based quantum computers made by chemistry: hows and whys. *J. Mater. Chem.* **2009**, *19*, 1718−1730.

(20) Evangelisti, M.; Brechin, E. K. Recipes for enhanced molecular cooling. *Dalton Trans* **2010**, *39*, 4672−4676.

(21) Troiani, F.; Affronte, M. Molecular spins for quantum information technologies. *Chem. Soc. Rev.* **2011**, *40*, 3119−3129.

(22) Timco, G. A.; Faust, T. B.; Tuna, F.; Winpenny, R. E. Linking heterometallic rings for quantum information processing and amusement. *Chem. Soc. Rev.* **2011**, *40*, 3067−3075.

(23) Dong, L.; Kumar, H.; Anasori, B.; Gogotsi, Y.; Shenoy, V. B. Rational Design of Two-Dimensional Metallic and Semiconducting Spintronic Materials Based on Ordered Double-Transition-Metal MXenes. *J. Phys. Chem. Lett.* **2017**, *8*, 422−428.

(24) Hellenbrandt, M. The inorganic crystal structure database (ICSD)present and future. *Crystallogr. Rev.* **2004**, *10*, 17−22.

(25) Holman, K.; Morosan, E.; Casey, P.; Li, L.; Ong, N.; Klimczuk, T.; Felser, C.; Cava, R. Crystal structure and physical properties of Mg6Cu16Si7-type M6Ni16Si7, for M= Mg, Sc, Ti, Nb, and Ta. *Mater. Res. Bull.* **2008**, *43*, 9−15.

(26) Spiegel, F.; Beck, P.; Bardos, D. Ternary G and E silicides and germanides of transition elements. *Trans. Metall. Soc. AIME* **1963**, *227*, 575−579.

(27) Chaudouet, P.; Madar, R.; Fruchart, R.; Lambert, B. Etude de nouveaux pnictures ternaires de metaux de transition isostructuraux des phases G, Ni16Mn6P7, Ni16Mn6As7. *Mater. Res. Bull.* **1983**, *18*, 713−719.

(28) Bowden, G.; Cadogan, J.; De Leon, H.; Ryan, D. The easy magnetization directions in R 6 Fe 23 intermetallic compounds: A crystal field analysis. *J. Appl. Phys.* **1997**, *81*, 4186−4188.

(29) Ostorero, J. Magnetic properties of (Ho, Y) 6Fe23 intermetallic compounds. *J. Alloys Compd.* **2001**, *317-318*, 450−454.

(30) Ostoréro, J.; Paul-Boncour, V.; Bourée, F.; André, G. Neutron diffraction study of Ho5YFe23 and Ho5YFe23D16 deuteride. *J. Alloys Compd.* **2005**, *404-406*, 191−194.

(31) Stadnik, Y.; Skolozdra, R. Magnetic-Properties of Me_6Ni_{16} (Si, Ge) 7 Compounds (Me-Transition Metals of IVA-VIIA Subgroups. *Ukr. Fiz. Zh.* **1983**, *28*, 1031−1035.

(32) Kolenda, M.; Szytuła, A.; Leciejewicz, J.; Maletka, C. Magnetic properties of Mn6 Ni16 Si7 and Mn3 Cr3 Ni16 Si7. *J. Magn. Magn. Mater.* **1991**, *96*, 121−124.

(33) Rodriguez-Carvajal, J. FullProf: a program for Rietveld refinement and pattern matching analysis. *Satellite Meeting on Powder Diffraction of the XV Congress of the IUCr*, 1990.

(34) Rodríguez-Carvajal, J. Recent developments of the program FullProf. *Commission on Powder Diffraction (IUCr) Newsletter* **2001**, *26*, 12−19.

(35) Rodríguez-Carvajal, J. *FullProf* 2k; *International Union for Crystallography*, 2011.

(36) Wills, A. A new protocol for the determination of magnetic structures using simulated annealing and representational analysis (SARAh). *Phys. B* **2000**, *276-278*, 680−681.

DOI: 10.1021/acs.inorgchem.8b01964
Inorg. Chem. XXXX, XXX, XXX−XXX

(37) Fisher, M. E. Relation between the specific heat and susceptibility of an antiferromagnet. *Philos. Mag.* **1962**, *7*, 1731−1743.
(38) Marjerrison, C. A.; Mauws, C.; Sharma, A. Z.; Wiebe, C. R.; Derakhshan, S.; Boyer, C.; Gaulin, B. D.; Greedan, J. E. Structure and Magnetic Properties of KRuO4. *Inorg. Chem.* **2016**, *55*, 12897−12903.
(39) Yan, X.; Grytsiv, A.; Rogl, P.; Pomjakushin, V.; Xue, X. On the crystal structure of the Mn−Ni−Si G-phase. *J. Alloys Compd.* **2009**, *469*, 152−155.
(40) Engelfriet, D.; Groeneveld, W.; Groenendijk, H.; Smit, J.; Nap, G. 1, 2, 4-Triazole Complexes VIII*. *Z. Naturforsch., A: Phys. Sci.* **1980**, *35*, 115−128.
(41) Carlin, R. L.; Joung, K. O.; Van Der Bilt, A.; Den Adel, H.; O'Connor, C. J.; Sinn, E. Structural and magnetic properties of Co (urea) 2Cl2 2H2O: A two-dimensional Ising system with hidden canting. *J. Chem. Phys.* **1981**, *75*, 431−439.
(42) Tian, Y.-Q.; Cai, C.-X.; Ren, X.-M.; Duan, C.-Y.; Xu, Y.; Gao, S.; You, X.-Z. The Silica-Like Extended Polymorphism of Cobalt (II) Imidazolate Three-Dimensional Frameworks: X-ray Single-Crystal Structures and Magnetic Properties. *Chem. - Eur. J.* **2003**, *9*, 5673−5685.
(43) Wang, X.-Y.; Wang, L.; Wang, Z.-M.; Su, G.; Gao, S. Coexistence of spin-canting, metamagnetism, and spin-flop in a (4, 4) layered manganese azide polymer. *Chem. Mater.* **2005**, *17*, 6369−6380.

DOI: 10.1021/acs.inorgchem.8b01964
Inorg. Chem. XXXX, XXX, XXX−XXX